Title:

Proteomic Immune Signatures of Severe HIV-Associated Tuberculosis in Sub-Saharan Africa: A Prospective, Multicenter Analysis from Uganda

Authors and Affiliations:

Jesse E. Ross MD,[1] Alin S. Tomoiaga PhD,[2] Nicholas Owor BA,[3] Xuan Lu MPH,[4] Joseph Shinyale RN,[5] Tonny Kiyingi MBChB,[3] Ignatius Asasira MBChB,[3] Peter James Eliku MS,[3] John Bosco Nsubuga MBChB,[5] Christopher Nsereko MBChB,[5] Irene Nayiga MBChB,[5] Stephen Kyebambe MBChB,[5] Thomas Ochar MBChB,[6] Moses Kiwubeyi DMLT,[6] Rittah Nankwanga RN,[6] Kai Nie MSc,[7] Hui Xie MSc,[7] Sam Miake-Lye MS,[7] Bryan Villagomez BS,[7] Jingjing Qi MS,[7] Steven J Reynolds MD,[8,9,10] Martina Cathy Nakibuuka MHS,[10] John Kayiwa MS,[3] Mercy Haumba BA,[3] Joweria Nakaseegu BS,[3] Xiaoyu Che PhD, [11] Risa Hoffman MD,[12] John A Belperio,[1] Julius J. Lutwama PhD,[3] Seunghee Kim-Schulze PhD,[7] Max R. O'Donnell MD,[4,11,13] Barnabas Bakamutumaho MBChB,[3,14†] Matthew J. Cummings MD[4,11†]

[1]Department of Medicine, Division of Pulmonary, Critical Care, Allergy, and Immunology, David Geffen School of Medicine at University of California, Los Angeles, CA, USA.

[2]Department of Accounting, Business Analytics, Computer Information Systems, and Law, Manhattan College, New York, USA

[3]Department of Arbovirology, Emerging and Re-emerging Infectious Diseases, Uganda Virus Research Institute, Entebbe, Uganda

[4]Department of Medicine, Division of Pulmonary, Allergy, and Critical Care Medicine, Vagelos College of Physicians and Surgeons, Columbia University, New York, NY, USA

[5]Entebbe Regional Referral Hospital, Ministry of Health, Entebbe, Uganda

[6]Tororo General Hospital, Ministry of Health, Tororo, Uganda

[7]Human Immune Monitoring Center, Icahn School of Medicine at Mount Sinai, New York, New York

[8]National Institute of Allergy and Infectious Diseases, National Institutes of Health, Bethesda, MD, USA

[9]Johns Hopkins University School of Medicine, Baltimore, MD, USA

[10]Rakai Health Sciences Program, Kalisizo, Uganda

[11]Center for Infection and Immunity, Mailman School of Public Health, Columbia University, New York, NY, USA

[12]Department of Medicine, Division of Infectious Diseases, David Geffen School of Medicine at University of California, Los Angeles, USA.

[13]Department of Epidemiology, Mailman School of Public Health, Columbia University, New York, NY, USA

[14]Immunizable Diseases Unit, Uganda Virus Research Institute, Entebbe, Uganda

†Co-senior authors

Corresponding Author: Jesse E Ross MD, MS, 200 UCLA Medical Plasa Ste 365B. Los Angeles CA, 90095-8344

Funding: This work was supported by the National Heart Lung and Blood Institute (5T32HL105323-08 to J.E.R), the National Institute of Allergy and Infectious Diseases (K23AI16334 and R01AI184997 to M.J.C and the Division of Intramural Research [S.J.R]), and the National Center for Advancing Translational Sciences (UL1TR001873 to Columbia University, sub-award to M.R.O), National Institutes of Health. Additional support was provided by the Burroughs Wellcome Fund /American Society of Tropical Medicine and Hygiene (M.J.C), the Potts Memorial Foundation (J.E.R), and the Stony Wold-Herbert Fund, Inc. (J.E.R). This research was support in part by the Intramural Research Program of the NIH. The contributions of the NIH author(s) were made as part of their official duties as NIH federal employees, are in compliance with agency policy requirements, and are considered Works of the United States Government. However, the findings and conclusions presented in this paper are those of the author(s) and do not necessarily reflect the views of the NIH or the U.S. Department of Health and Human Services.

Abstract

Background: Severe tuberculosis (TB) is a major cause of critical illness and death in people living with HIV (PLWH) worldwide. Despite this, the immunopathology of severe HIV-associated TB (HIV/TB) is poorly understood. We aimed to identify an immunopathologic signature of severe HIV/TB in sub-Saharan Africa.

Setting: We analyzed proteomic data from two prospective observational cohorts of adults hospitalized with severe undifferentiated infection in Uganda: an urban discovery cohort (Entebbe, N=241) and a rural validation cohort (Tororo, N=253).

Methods: Soluble immune-related proteins were quantified in serum using Olink proteomics. Participants were stratified into three HIV/TB phenotypes: HIV-negative without TB, PLWH without TB, and PLWH with microbiologically diagnosed TB. We applied ordinal random forest models in the discovery cohort to identify proteins strongly predictive of progressive HIV/TB phenotype. The top 10 ranked proteins were then analyzed using multivariable linear regression models in both the discovery and validation cohorts to quantify their associations with HIV/TB phenotype.

Results: In both cohorts, PLWH with microbiologically diagnosed TB were at highest risk of physiological instability and death. An eight-protein signature reliably distinguished this phenotype, reflecting mediators of macrophage/dendritic cell activation (LAMP3), NK- and T-cell stimulation and cytotoxicity (CD70, CRTAM), B-cell activation (IGLC2), protease-mediated tissue injury (PRSS2), dysregulated coagulation (SERPINA5), extracellular matrix remodeling (EFEMP1), and GH/IGF axis dysregulation (IGFBP3).

Conclusions: We identified an immunologic signature of severe HIV-associated TB defined by mediators of macrophage/dendritic cell and cytotoxic lymphocyte activation, extracellular matrix remodeling, and dysregulated coagulation. These findings offer new insight into HIV/TB pathobiology and highlight potential targets for host-directed therapies in this high-risk population.

Introduction:

Severe tuberculosis (TB) is the leading cause of hospitalization and death among people living with HIV (PLWH) globally, with the highest TB burden in low- and middle-income countries (1–4). In sub-Saharan Africa (SSA), where HIV and TB are co-epidemic, MTB is the predominant cause of critical illness and death among hospitalized PLWH (5–6). In

90 this population, the frequency of disseminated MTB infection can exceed 40%, with short-
91 term mortality approaching 50% (6–9).

92 Despite this substantial burden, the immunopathology of severe HIV-associated
93 tuberculosis (HIV/TB) remains poorly understood. Few studies have characterized
94 multidimensional host responses in PLWH with severe TB, limiting insight into the
95 mechanisms driving immune dysfunction in this critically ill population and, consequently,
96 limiting the ability to target specific treatment mechanisms that may improve outcomes (1,
97 10 – 17). Available data suggests that MTB infection may be linked to activation of both
98 pro- and anti-inflammatory innate immune pathways, dysregulated T-cell activation and
99 exhaustion, endothelial dysfunction, and extracellular matrix remodeling (1, 10–17),
100 features that partially overlap with those observed in both HIV and critically ill patients
101 with non-TB bacterial infections (18–20). However, most studies to date have relied on
102 narrow biomarker panels, single-center designs, and lacked comparator groups such as
103 HIV-uninfected and TB-negative controls, which reduces immunologic resolution, hinders
104 attribution of TB-specific responses versus HIV or other critical illness, and limits
105 generalizability across settings (1, 10 – 17). Concurrently, emerging evidence from other
106 severe infections underscores substantial heterogeneity in host immune responses, shaped
107 not only by the pathogen but also by host-specific factors such as comorbidities and
108 immune status (19–21). In PLWH, chronic immune activation, T-cell exhaustion, and
109 endothelial dysfunction further influence host-pathogen interactions, potentially giving rise
110 to distinct immunopathologic signatures of critical illness (23–28). This biological
111 complexity underscores the need for higher-resolution immune profiling in severe
112 HIV/TB.

113 To address these gaps, we conducted high-throughput serum proteomic profiling in two
114 prospective hospital-based cohorts in Uganda to identify a reproducible immune signature
115 of severe HIV-associated TB. We hypothesized that hospitalized PLWH with severe TB
116 would exhibit a reproducible serum proteomic signature reflecting exaggerated innate
117 immune activation and T-cell exhaustion.

118 # Methods

119 **Study Settings, Outcomes, and Participants**

120 We analyzed data from two prospective observational cohorts of adults hospitalized with
121 severe febrile illness at two public hospitals in Uganda (**Figure 1**). The discovery cohort
122 (RESERVE-U-1-EBB) was enrolled at Entebbe Regional Referral Hospital (ERRH), an
123 urban referral hospital in central Uganda, between April 2017 and August 2019. The
124 validation cohort (RESERVE-U-2-TOR) was enrolled at Tororo General Hospital (TGH),
125 a rural district hospital in eastern Uganda, between November 2021 and August 2023.
126 Enrollment criteria were uniform across the RESERVE-U cohorts. Non-pregnant adults
127 (age ≥18 years) hospitalized with severe febrile illness (i.e., severe undifferentiated
128 infection) were enrolled based on a reported history of fever or axillary temperature ≥
129 37.5°C and illness severe enough to warrant admission. The primary clinical outcomes for
130 RESERVE-U-1-EBB and RESERVE-U-2-TOR were 30- and 60-day vital status,
131 respectively. Details of these cohorts have been published and are included in the
132 supplement along with further details of study sites, procedures, and outcomes (18).
133

134 **Study Procedures**

135 Enrolled participants underwent standardized clinical assessments, including rapid testing
136 for HIV by a Ministry of Health-recommended algorithm (29) and pathogens implicated
137 as etiologies of severe infection in SSA, as informed by World Health Organization (WHO)
138 guidelines (28). For PLWH, MTB testing included Xpert MTB/RIF Ultra (Cepheid,
139 Sunnyvale, CA, USA) on sputum samples and Determine TB-LAM (Abbott/Alere, Lake
140 Bluff, IL, USA) on urine samples, where specimens were obtainable. TB testing of patients
141 without HIV was at the discretion of treating clinicians.
142

143 Participants from both cohorts were individually categorized into one of three ordinal
144 groups reflecting HIV/TB co-infection phenotypes: (1) HIV-negative and TB-negative
145 (HIV-/TB-), (2) HIV-positive and TB-negative (HIV+/TB-), (3) HIV-positive and TB-
146 positive (HIV+/TB+). Microbiological diagnosis of TB was based on a positive sputum
147 Xpert MTB/RIF Ultra or urine TB-LAM result. HIV-uninfected participants were
148 classified at TB-negative if sputum Xpert MTB/RIF Ultra was negative and there was no

149 clinical suspicion of TB. PLWH were classified as TB-negative if both sputum Xpert
150 MTB/RIF Ultra and urine TB-LAM results were negative and there was no clinical
151 suspicion of TB. In both cases, no clinical suspicion of TB was defined as the treating
152 clinicians' decision not to initiate empiric anti-TB therapy. Serum samples were collected
153 at the time of study enrollment and stored at –80°C until the time of analysis.
154
155 **Olink Proteomics**
156 Proteomic profiling was performed on cryopreserved serum samples using the Olink Target
157 Immunooncology and Cardiometabolic panels (Olink Proteomics AB, Uppsala, Sweden),
158 which together quantify concentrations of 184 soluble proteins (18). These panels were
159 utilized to capture multiple biological domains implicated in the host response to severe
160 infection (i.e., innate and adaptive immune activation, endothelial dysfunction, and
161 dysregulated coagulation), including severe TB. For each panel, proteins were quantified
162 via the Olink Proximity Extension Assay (PEA) platform, and relative protein abundance
163 was expressed in $\log_2$ normalized protein expression (NPX) units. Proteins were excluded
164 from downstream analyses if <20% of NPX values were above each panel's estimated limit
165 of detection (18).
166
167 **Biomarker Selection Using Ordinal Forest Models**
168 To identify soluble proteins associated with HIV/TB phenotypes, we applied an ordinal
169 random forest model to the RESERVE-U-1-EBB discovery cohort, using the three-level
170 HIV/TB phenotype classification as the ordinal outcome. To mitigate class imbalance and
171 optimize feature selection across all HIV/TB phenotypes, we performed class-balanced
172 upsampling through duplicating existing minority class samples, thereby equalizing group
173 representation during model training. Upsampling was restricted to the training data within
174 each resampling split, and the independent validation set was never upsampled. Random
175 forest model parameters included mtry = 5, nsets = 500, ntreeperdiv = 100, and nbest = 20.
176 The predictive strength of each protein was quantified using permutation-based variable
177 importance. The top ten proteins were selected from the importance rankings to provide a
178 parsimonious set of features that balances model interpretability with sufficient depth for
179 downstream analyses.

180

181 **Multivariable Analysis of Soluble Proteins and HIV/TB Phenotypes**

182 To quantify associations between soluble proteins and HIV/TB phenotypes, we analyzed
183 the top 10 proteins identified in the RESERVE-U-1-EBB discovery cohort using separate
184 multivariable linear regression models. Each model included NPX-quantified protein
185 expression as the continuous outcome and HIV/TB phenotype as an ordinal predictor.
186 Models were adjusted for age, sex, illness duration prior to enrollment, and malaria status.
187 To avoid collider bias, we did not adjust for physiological severity, which may be
188 influenced by both HIV/TB infection and host responses. We reported regression
189 coefficients, 95% confidence intervals, and p-values for linear trend, correcting the latter
190 for multiple testing using the Benjamini-Hochberg false discovery rate (FDR) method.
191 Proteins with FDR-adjusted p-values <0.05 in the RESERVE-U-1-EBB discovery cohort
192 were carried forward for testing in the RESERVE-U-2-TOR validation cohort using
193 identical regression models.

194

195 To explore whether proteomic associations with HIV/TB phenotypes were independent of
196 HIV-related immunosuppression and/or viremia, we conducted a sensitivity analysis
197 restricted to PLWH in the RESERVE-U-2-TOR cohort. We fit multivariable linear
198 regression models for each of the top ten proteins, with NPX-quantified protein expression
199 as the continuous outcome and HIV/TB phenotype as the ordinal predictor, adjusted for
200 CD4 count and HIV-1 viral load. CD4 count was modeled as a continuous variable while
201 HIV-1 viral load was modeled as a binary indicator: suppressed versus unsuppressed.
202 Details of CD4 count and HIV-1 viral load quantification methods have been described
203 and are in the supplement (**Table S1**) (18). Age, sex, illness duration, and malaria status
204 were not included in this model to prevent overfitting and underpowering of this HIV-
205 restricted exploratory analysis. Similarly, given the smaller sample size and exploratory
206 intent, FDR correction was not applied and unadjusted p-values are reported. CD4 count
207 and HIV-1 viral load data were unavailable from RESERVE-U-1-EBB participants.

208

209 All analyses were conducted in R version 4.3.2 using the tidyverse, ordinalForest, caret,
210 stats, broom, and patchwork packages.

211

212 **Ethics Statement**

213 Each enrolled participant or their surrogate provided written informed consent. Study
214 protocols were approved by ethics committees at Columbia University (AAAR1450),
215 Uganda Virus Research Institute (GC/127/17/02-06/582), and Uganda National Council
216 for Science and Technology (HS2308).

217

218 **Results**

219 *Participant Characteristics*

220 A total of 494 participants were analyzed: 241 in the RESERVE-U-1-EBB (discovery)
221 cohort and 253 in the RESERVE-U-2-TOR (validation) cohort. Characteristics of analyzed
222 patients stratified by HIV/TB phenotype are presented in **Tables 1 and 2.** Approximately
223 half of participants were female. The median age was 32 years (IQR 26 – 40) in Entebbe
224 and 48 years (IQR 33 – 61) in Tororo. The proportion of PLWH was similar in Entebbe
225 and Tororo (51% versus 50% respectively), though the proportion of PLWH receiving anti-
226 retroviral therapy was higher in Tororo (83% versus 68%). In PLWH enrolled in
227 RESERVE-U-2-TOR, the median CD4 count was 350 cells/μL (IQR 300-600) and 71%
228 had suppressed HIV-1 viral loads (<150 copies/mL). The frequency of microbiologically
229 diagnosed TB was similar across sites: 21% in Tororo and 18% in Entebbe. Among those
230 with microbiologically diagnosed TB, disseminated disease as indicated by positive urine
231 TB-LAM testing was present in 40/47 (85%) of PLWH in Entebbe and 51/53 (96%) of
232 PLWH in Tororo. Mortality at 30- and 60-days was 22% in RESERVE-U-1-EBB and 26%
233 in RESERVE-U-2-TOR, respectively. Most deaths occurred after hospital discharge. In
234 both cohorts, PLWH with microbiologically diagnosed TB were at highest risk of
235 physiological instability and death.

236 *Biomarker Results*

237 After excluding 11 proteins due to high proportions of expression values below each Olink
238 panel's estimated limits of detection, we applied an ordinal random forest model in the
239 RESERVE-U-1-EBB discovery cohort to 173 soluble proteins. The top ten most important
240 proteins for prediction of HIV/TB phenotype reflected macrophage and dendritic cell

241 activation (LAMP3), NK and T-cell stimulation and cytotoxic function (CD70, CRTAM,
242 IL-18), B cell activation and immunoglobulin production (IGLC2), protease-mediated
243 tissue injury (PRSS2), dysregulated coagulation (SERPINA5), leukocyte adhesion and
244 immune cell trafficking (ICAM3), extracellular matrix remodeling (EFEMP1), and growth
245 hormone (GH) / insulin-like growth factor (IGF) axis dysregulation (IGFBP-3) (**Figure 2**).
246
247 In the RESERVE-U-1-EBB discovery cohort, all ten proteins were significantly associated
248 with HIV/TB co-infection phenotype in multivariable linear regression models, including
249 after FDR adjustment (**Figure 3A, Table S2**). Expression levels of eight proteins increased
250 across the HIV-/TB-, HIV+/TB-, and HIV+/TB+ groups, while SERPINA5 and IGFBP-3
251 demonstrated an inverse association, with lower expression in participants with severe
252 HIV/TB. In the validation cohort (RESERVE-U-2-TOR), eight of the ten proteins
253 remained significantly associated with HIV/TB co-infection phenotype (**Figure 3B, Table**
254 **S3**); associations for IL-18 and ICAM3 did not reach statistical significance. Visual
255 inspection of boxplots confirmed consistent expression gradients across the HIV-/TB-,
256 HIV+/TB-, and HIV+/TB+ groups in both cohorts (**Figures 4A and 4B**), with the most
257 pronounced patterns observed for SERPINA5, LAMP3, and PRSS2.
258
259 In exploratory linear regression models restricted to PLWH in RESERVE-U-2-TOR and
260 adjusted for CD4 count and HIV-1 viral load (N = 127), three proteins, EFEMP1, IGLC2,
261 and SERPINA5, remained significantly associated with HIV/TB co-infection phenotype
262 (**Figure 5, Table S4**).

263 ## Discussion

264 We identified and validated a proteomic immune signature associated with clinical
265 phenotypes of HIV/TB in severely ill hospitalized adults in Uganda. To our knowledge,
266 this is the first multicenter study in SSA to apply high-throughput proteomics to define and
267 validate an immune signature of severe HIV-associated TB. These results advance
268 translational understanding of immune dysregulation in a leading cause of critical illness
269 and death among PLWH in the region. They also provide a foundation for biologically-

270 driven stratification of severe HIV-associated TB and could inform the design of
271 biomarker-guided treatment strategies for this high-risk population.

272 Our findings align with contemporary models of TB pathogenesis that emphasize the
273 balance between protective and pathological inflammation (30, 31). In the context of HIV,
274 loss and dysfunction of CD4 T cells and antigen-presenting cells (APCs) compromise
275 immune containment, permitting bacillary dissemination and multiorgan injury (30, 31).
276 The immune signature identified in our study supports this framework with *in vivo* data
277 from the global HIV/TB epicenter: LAMP3 reflects maturation/activation of macrophages
278 and dendritic cells and heightened antigen presentation; CD70 and CRTAM reflect
279 cytotoxic lymphocyte stimulation and potential exhaustion; IGLC2 denotes B-cell
280 activation and heightened humoral response; PRSS2 and EFEMP1 implicate proteolytic
281 tissue injury and extracellular matrix remodeling; lower SERPINA5 is consistent with
282 unrestrained serine-protease activity and coagulation dysregulation leading to an immune-
283 thrombotic milieu; and lower IGFBP-3 is associated with GH/IGF axis dysregulation, a
284 pattern previously reported with AIDS-associated wasting and increasing severity of sepsis
285 (32, 33). Collectively, these features define a reproducible HIV/TB signature linking APC
286 activation, cytotoxic and humoral lymphocyte stimulation, tissue injury, disordered
287 coagulation, and GH/IGF-axis perturbation.

288 Prior studies from South Africa have highlighted the complexity of immune dysregulation
289 in PLWH with severe TB, characterized by simultaneous activation and exhaustion across
290 innate and adaptive pathways (1, 11, 15). Using relatively low-dimensional cytokine
291 profiling, one study showed that non-survivors exhibited elevated concentrations of both
292 pro-inflammatory (CSF-3, TNF, IL-6) and anti-inflammatory (IL-1Ra) cytokines,
293 alongside expansion of pro-inflammatory monocytes but impaired capacity of innate cells
294 to mount cytokine responses to bacterial antigens (15). Broader cytokine panels have
295 identified a clinically high-risk profile dominated by innate and chemotactic mediators (IL-
296 6, IL-1Ra), whereas T-cell–associated mediators were inversely correlated with mortality
297 (1). More recently, anemia, upregulation of matrix metalloproteinases (MMPs), and
298 extracellular matrix turnover have also been linked with disease severity and poor
299 outcomes in severe HIV/TB (11, 13).

300 A complementary study from South Africa in PLWH quantified circulating MTB burden
301 using blood-based Xpert MTB/RIF Ultra and demonstrated a dose–response relationship
302 between bacillary load, host-response signatures of inflammation and tissue damage, and
303 mortality risk (12). Related work from our group in Uganda showed that higher urine TB-
304 LAM grade, a marker of bacillary burden, was significantly associated with increased pro-
305 inflammatory innate and T-cell activation and chemotaxis (10). Building on these findings,
306 our 173-protein analysis provides a higher-resolution view of HIV/TB pathogenesis,
307 revealing axes of immune dysregulation not captured by narrower cytokine panels.
308 Specifically, we implicate APC activation (LAMP3), humoral activation (IGLC2), and
309 cytotoxic-cell signaling (CD70, CRTAM), alongside extracellular matrix damage
310 (EFEMP1), tissue injury (PRSS2), coagulation dysregulation (SERPINA5), and GH/IGF
311 pathway disruption thereby extending the paradigm beyond pathogen load and broad
312 inflammatory markers toward a more integrated host–pathogen framework. Additionally,
313 our work demonstrates external validation across two hospitals with HIV-negative and TB-
314 negative comparators, improving dissection of HIV/TB-specific biology across the clinical
315 spectrum. Together, these findings point to a coordinated and multifaceted host response
316 involving both innate and adaptive pathways, building on prior studies implicating immune
317 activation in TB severity and poor outcomes among PLWH. In conjunction with pathogen-
318 centric work, this motivates a combined pathogen-load plus host-response staging
319 framework to inform risk stratification and potentially therapeutic trial design in severe
320 HIV/TB.

321 Across the clinical spectrum of HIV/TB co-infection, the respective contributions of HIV
322 and MTB to immune dysregulation, including mechanisms that drive illness severity,
323 remain poorly defined (31, 34). Prior studies from South Africa have shown that HIV
324 viremia and CD4 lymphocytopenia are associated with host inflammatory responses, with
325 IL-17A, which was not included in our Olink panels, emerging as a central immunological
326 mediator (30, 31, 34). In contrast, a prior study from Malawi showed that blunted TNF
327 production in monocytes, suggesting innate immunoparalysis, was strongly predictive of
328 poor outcomes in severe TB while HIV co-infection was not (17). In an exploratory
329 analysis restricted to PLWH in the RESERVE-U-2-TOR cohort, three proteins reflecting
330 B-cell activation and immunoglobulin production (IGLC2), dysregulated coagulation

331 (SERPINA5), and extracellular matrix remodeling (EFEMP1) remained significantly
332 associated with HIV/TB phenotype after adjustment for CD4 count and HIV-1 viral load.
333 These persistent associations suggest that although HIV-related immunosuppression and/or
334 viremia may contribute to immune dysregulation observed in our cohorts, it does not fully
335 account for the proteomic signature observed in severe HIV/TB. Nonetheless, given the
336 exploratory nature of this analysis, our results should be interpreted cautiously and
337 considered hypothesis-generating.

338 Beyond identifying an immune signature of severe HIV/TB, our findings advance
339 understanding of TB-specific immune responses, in contrast to those observed in other
340 severe HIV-associated infections (18–20). Prior analyses of the RESERVE-U cohorts
341 identified two pathobiologically-driven "Uganda Sepsis Signatures" (USS-1/USS-2), with
342 USS-2, enriched for severe HIV/TB and higher mortality, defined by myeloid cell and
343 inflammasome activation, T-cell exhaustion, endothelial barrier dysfunction and
344 prothrombotic imbalance (18). Our findings build on these insights, suggesting the
345 presence of a reproducible immunopathological signature specific to severe HIV-
346 associated TB in the global sepsis epicenter.

347 Our findings have direct relevance for the development of host-directed therapeutics in
348 severe HIV/TB. As diagnostic capabilities expand, protein-based signatures such as ours
349 could enable precise, biomarker-guided treatment strategies and support the design of
350 immunomodulatory treatment trials (12, 35). Several candidate therapies are already being
351 evaluated, including in randomized controlled trials. For example, corticosteroids in
352 NewStrat-TB aim to attenuate hyperinflammatory immune activation; doxycycline, a
353 known MMP inhibitor, may mitigate matrix injury and remodeling, as suggested by
354 preclinical and phase 2 data; aspirin targets the immunothrombotic axis, with signals of
355 safety and potential benefit demonstrated in TB meningitis (11, 36–39). Conceptually, a
356 parsimonious protein signature could be operationalized to enrich randomization in
357 ongoing or future host-directed treatment trials and serve as an early biomarker endpoint.
358 Moving forward, combining longitudinal proteomic profiling with quantitative pathogen
359 measurements could jointly stage bacillary burden and host response. In a serial sampling
360 study of disseminated HIV-associated TB, MTB DNA remained detectable in blood and

361 urine for up to 14 days after therapy initiation (40), underscoring the sustained
362 disseminated burden early in treatment and the potential value of pairing dynamic pathogen
363 and host-response data to refine therapeutic strategies.

364 Our study has several strengths. Our primary analysis was performed in two independent
365 prospective cohorts, across distinct geographic and temporal settings, encompassing nearly
366 500 hospitalized adults. These cohorts reflect real-world clinical populations at high risk
367 for HIV/TB co-infection and mortality, enhancing the translational relevance of our
368 findings. We employed a tiered analytical approach combining robust machine learning–
369 based feature selection with prespecified multivariable models and validation. By treating
370 HIV/TB phenotype as an ordinal variable, our models captured gradations in clinical and
371 microbiological phenotypes, rather than relying on binary group comparisons. Predictive
372 associations largely held across cohorts, increasing generalizability in high-burden
373 settings. The Olink platform enabled relatively high-throughput measurement of soluble
374 proteins across multiple biological domains. Importantly, several proteins retained
375 significant associations even after adjustment for CD4 count and viral load, suggesting
376 components of the signature reflect TB-specific immunopathology. Together, these
377 strengths support the biological plausibility, scalability, and external validity of the
378 identified immune signature.

379 Our study also has limitations. Although the two cohorts were geographically and
380 temporally distinct, we did not conduct external validation outside Uganda. However,
381 participant characteristics were broadly comparable to those of comparable cohorts in SSA
382 (41). While we included only microbiologically confirmed TB cases in the HIV+/TB+
383 group, undiagnosed or subclinical TB may have been present in the HIV-/TB- and
384 HIV+/TB- groups, potentially resulting in misclassification and attenuation of observed
385 differences biasing results towards the null. Although we attempted to adjust for co-
386 infections where data were available, including malaria, adjustment for cryptococcal and
387 other bacterial infections was not possible due to limited testing. Blood cultures were not
388 performed because of resource limitations. Therefore, residual confounding from
389 unmeasured or incompletely characterized infections is possible, and our signature may
390 reflect a more complex infectious background not limited to TB and HIV. We also did not

include a direct measure of circulating mycobacterial burden, which could have strengthened our interpretation of immune activation patterns. Additionally, CD4 count and HIV-1 viral load data were only available in the RESERVE-U-2-TOR cohort, limiting adjustment for HIV disease severity in the discovery cohort. CD4 counts were multiply imputed in a proportion of PLWH in RESERVE-U-2-TOR (18). However, we believe this approach is justified, as simulation studies have demonstrated that multiple imputation reduces bias compared to complete case analysis, even at higher levels of missingness than our CD4 data (42). Proteomic data were collected at a single time point, which limits our ability to assess dynamic immune responses over the course of illness or treatment. Finally, our analysis focused on soluble protein expression, which may not fully reflect tissue-level immune processes, particularly in lung or intra-cellular compartments central to TB pathogenesis. Moreover, the Olink platform provides relative (NPX) assessments of protein expression rather than absolute quantification, which may limit cross-platform comparability.

In conclusion, we identified a reproducible eight-protein immune signature associated with HIV/TB co-infection among severely ill hospitalized adults in Uganda. These findings provide new insights into the immunopathology of severe HIV/TB in this high-risk population and highlight potential candidate biomarkers that could support future prognostic and therapeutic research.

<u>Author Contributions</u>

JER, BB, MRO'D, and MJC conceived the study and design. JJL, NO, CN, IN, SK, TO, MK, RN, JK, MH, and JN collected, organized and entered clinical data and blood samples and contributed to pathogen diagnostics. SKS, KN, HX, SML, BV contributed to proteomic analyses. JER, MJC, AT, and XL had full access to all data in the study and contributed to data cleaning, processing, verification, and analysis. JER developed the first draft of the manuscript. JER, AT, NO, XL, JS, TK, IA, PJE, JBN, CN, IN, SK, TO, MK, RN, KN, HX, SML, BV, JQ, SJR, MCN, JK, MH, JN, XC, WIL, RH, JAP, JJL, SKS, MRO, BB, MJC reviewed and edited the final version of the manuscript. JER had final responsibility for the decision to submit for publication.

420 Declaration of Interests

421 MJC reports consulting fees from Vertex Pharmaceuticals and Veracyte unrelated to the
422 submitted work. The remaining authors declare no conflicts of interest.

423 Data sharing

424 Proteomic data are available in Dryad at https://doi.org/10.5061/dryad.b2rbnzsq2. Analytic
425 code will be deposited in Github prior to publication.

426

427

428

429

430

431

432

433

434

435

436 **References**

437 1. Schutz C, Barr D, Andrade B, et al. Clinical, microbiologic, and immunologic determinants of
438 mortality in hospitalized patients with HIV-associated tuberculosis: a prospective cohort study.
439 *PLoS Med*. 2019;16(7): e1002840.
440 2. UNAIDS. Fact sheet—World Tuberculosis Day 2022. Geneva, Switzerland: Joint United Nations
441 Programme on HIV/AIDS; 2022. Available at: https://www.unaids.org.
442 3. Ford N, Matteelli A, Shubber Z, et al. TB as a cause of hospitalization and in-hospital mortality
443 among people living with HIV worldwide: a systematic review and meta-analysis. *J Int AIDS Soc.*
444 2016;19(1):20714.
445 4. World Health Organization. Global tuberculosis report 2022. Geneva, Switzerland: World Health
446 Organization; 2022. Available at: https://www.who.int.

5. Rudd K, Johnson S, Agesa K, et al. Global, regional, and national sepsis incidence and mortality, 1990–2017: analysis for the Global Burden of Disease Study. *Lancet.* 2020;395:200–211.
6. Cummings M, O'Donnell M. Inverting the pyramid: increasing awareness of mycobacterial sepsis in sub-Saharan Africa. *Int J Tuberc Lung Dis.* 2015;19(10):1128–1134.
7. Reddy E, Shaw A, Crump J. Community-acquired bloodstream infections in Africa: a systematic review and meta-analysis. *Lancet Infect Dis.* 2010;10(6):417–32.
8. Barr D, Lewis J, Feasey N, et al. *Mycobacterium tuberculosis* bloodstream infection prevalence, diagnosis, and mortality risk in seriously ill adults with HIV: a systematic review and meta-analysis of individual patient data. *Lancet Infect Dis.* 2020;20(6):742–752.
9. Gupta R, Lucas S, Fielding K, et al. Prevalence of tuberculosis in post-mortem studies of HIV-infected adults and children in resource-limited settings: a systematic review and meta-analysis. *AIDS.* 2015;29(15):1987–2002.
10. Cummings M, Bakamutumaho B, Jain K, et al. Detection of urine lipoarabinomannan is associated with proinflammatory innate immune activation, impaired host defense, and organ dysfunction in adults with severe HIV-associated tuberculosis in Uganda. *J Acquir Immune Defic Syndr.* 2023;93(1):79–85.
11. Walker N, Schutz C, Ward A, et al**.** Elevated plasma matrix metalloproteinases associate with *Mycobacterium tuberculosis* bloodstream infection and mortality in HIV-associated tuberculosis. *J Infect Dis.* 2025;231(1):109–114
12. Boloko L, Schutz C, Sibiya N, et al. Xpert Ultra testing of blood in severe HIV-associated tuberculosis to detect and measure *Mycobacterium tuberculosis* bloodstream infection: a diagnostic and disease biomarker cohort study. *Lancet Microbe.* 2022;3(7):e521–e532.
13. Araújo-Pereira M, Schutz C, Barreto-Duarte B, et al. Interplay between systemic inflammation, anemia, and mycobacterial dissemination and its impact on mortality in TB-associated HIV: a prospective cohort study. *Front Immunol.* 2023;14:1177432.
14. Ravimohan S, Tamuhla N, Steenhoff A, et al. Immunological profiling of tuberculosis-associated immune reconstitution inflammatory syndrome and non-IRIS death in HIV-infected adults with pulmonary tuberculosis starting antiretroviral therapy: a prospective observational cohort study. *Lancet Infect Dis.* 2015;15(4):429–438.
15. Janssen S, Schutz C, Ward A, et al**.** Mortality in severe human immunodeficiency virus–tuberculosis associates with innate immune activation and dysfunction of monocytes. *Clin Infect Dis.* 2017;65(1):73–82.
16. Clark D, Banura P, Bandeen-Roche K, et al. Biomarkers of endothelial activation/dysfunction distinguish subgroups of Ugandan patients with sepsis and differing mortality risks. *JCI Insight.* 2019;5(10):e127623.
17. Waitt C, Banda N, White S, et al. Early deaths during tuberculosis treatment are associated with depressed innate responses, bacterial infection, and tuberculosis progression. *J Infect Dis.* 2011;204(3):358–62.
18. Cummings M, Lutwama J, Owor N, et al. Unsupervised classification of the host response identifies dominant pathobiological signatures of sepsis in sub-Saharan Africa. *Am J Respir Crit Care Med.* 2025;211(3):357–369.
19. Reddy K, Sinha P, O'Kane C, et al. Subphenotypes in critical care: translation into clinical practice. *Lancet Respir Med.* 2020;8(6):631–643.
20. van der Poll T, Shankar-Hari M, Wiersinga W. The immunology of sepsis. *Immunity.* 2021;54(11):2450–2464
21. Singer M, Deutschman C, Seymour C, et al. The third international consensus definitions for sepsis and septic shock (Sepsis-3). *JAMA.* 2016;315:801–810.
22. Schutz C, Meintjes G, Almajid F, et al. Clinical management of tuberculosis and HIV-1 co-infection. *Eur Respir J.* 2010;36(6):1460–81.
23. Kanmogne GD. HIV infection, antiretroviral drugs, and the vascular endothelium. *Cells.* 2024;13(8):672.
24. Mu W, Patankar V, Kitchen S, et al. Examining chronic inflammation, immune metabolism, and T cell dysfunction in HIV infection. *Viruses.* 2024;16(2):219.

25. Walker N, Meintjes G, Wilkinson R. HIV-1 and the immune response to TB. *Future Virol.* 2013;8(1):57–80.
26. Cummings M, Bakamutumaho B, Price A, et al. HIV infection drives pro-inflammatory immunothrombotic pathway activation and organ dysfunction among adults with sepsis in Uganda. *AIDS.* 2023;37:233–245.
27. Hunt P, Lee S, Siedner M. Immunologic biomarkers, morbidity, and mortality in treated HIV infection. *J Infect Dis.* 2016;214(Suppl 2):S44–S50.
28. World Health Organization. IMAI district clinician manual: hospital care adolescents and adults. Geneva, Switzerland: World Health Organization; 2012. Available at: https://www.who.int/publications/i/item/imai-district-clinician-manual-hospital-care-adolescents-and-adults.
29. Ministry of Health. National HIV Testing Services Policy and Implementation Guidelines: Uganda. 4th Edition. October 2016. Available at: https://library.health.go.ug/sites/default/files/resources/UGANDA%20HTS%20POLICY%20AND%20IMPLEMENTATION%20GUIDELINES%202016%20%282%29.pdf
30. Scriba T, Maseeme M, Young C, et al. Immunopathology in human tuberculosis. *Sci Immunol.* 2024;9(102):eado5951.
31. Meintjes G, Maartens G**.** HIV-associated tuberculosis. *N Engl J Med.* 2024;391(4):343–355.
32. Frost R, Fuhrers J, Steigbigels R, et al. Wasting in the acquired immune deficiency syndrome is associated with multiple defects in the serum insulin-like growth factor system. *Clinical Endocrinology.* 1996;44:501-514
33. Papastathi C, Mavrommatis A, Mentzelopoulos S, et al. Insulin-like growth factor I and its binding protein 3 in sepsis. *Growth Hormone & IGF Research*. 2013;23(4):98-104.
34. Du Bruyn E, Fukutani K, Rockwood N, et al. Inflammatory profile of patients with tuberculosis with or without HIV-1 co-infection: a prospective cohort study and immunological network analysis. *Lancet Microbe.* 2021;2(8):e375–e385.
35. Ross J, Cummings M, Bakamutumaho B, et al. Xpert MTB/RIF Ultra enables sensitive detection of *Mycobacterium tuberculosis* in blood. *Int J Tuberc Lung Dis.* 2024;28(12):594–596.
36. Namale P, Boloko L, Vermeulen M, et al. Testing novel strategies for patients hospitalised with HIV-associated disseminated tuberculosis (NewStrat-TB): protocol for a randomised controlled trial. *Trials.* 2024;25(1):311.
37. Miow Q, Vallejo A, Wang Y, et al. Doxycycline host-directed therapy in human pulmonary tuberculosis. *J Clin Invest.* 2021;131(15):e141895.
38. Walker N, Clark S, Oni T, et al. Doxycycline and HIV infection suppress tuberculosis-induced matrix metalloproteinases. *Am J Respir Crit Care Med.* 2012;185(9):989–997.
39. Rohilla R, Shafiq N, Malhotra S. Efficacy and safety of aspirin as an adjunctive therapy in tubercular meningitis: a systematic review and meta-analysis. *EClinicalMedicine.* 2021;34:100819.
40. Boloko L, Vermeulen M, Sossen B, et al. Blood and urine early treatment response biomarkers in HIV-associated disseminated tuberculosis. *S Afr J HIV Med.* 2025;26(1):1664.
41. Lewis JM, Feasey NA, Rylance J. Aetiology and outcomes of sepsis in adults in sub-Saharan Africa: a systematic review and meta-analysis. *Crit Care.* 2019;23:212.
42. Madley-Dowd P, Hughes R, Tilling K, et al. The proportion of missing data should not be used to guide decisions on multiple imputation. *J Clin Epidemiol.* 2019;110:63–73.

546 **Table 1: Participant characteristics stratified by HIV/TB phenotype in RESERVE-**
547 **U-1-EBB cohort.**

Characteristics [a]	All participants N = 241	HIV - / TB - N = 117	HIV + / TB - N = 77	HIV + / TB + N=47
Demographics				
Female sex	149/241 (62%)	71/117 (61%)	52/77 (68%)	26/47 (55%)
Age, years	32 (26, 40)	28 (23, 38)	37 (30, 43)	32 (27, 40)
Mid-upper arm circumference, cm	--	--	--	--
Illness duration prior to enrollment, days	4 (2, 6)	3 (2, 5)	4 (3, 7)	6 (3, 7)
Clinical signs and physiological severity scores				
KPS at hospital admission	--	--	--	--
Whole-blood lactate, mmol/L	--	--	--	--
qSOFA score ≥ 2[b]	139/241 (58%)	87/117 (74%)	38/77 (49%)	14/47 (30%)
Modified Early Warning Score	3 (2, 4)	3 (2, 3)	3 (2, 4)	5 (3, 6)
Universal Vital Assessment score	2 (1, 4)	1 (0, 2)	3 (2, 5)	3 (3, 7)
HIV Characteristics				
PLWH	124/241 (51%)	NA	77/77 (100%)	47/47 (100%)
WHO HIV clinical stage 3 or 4	97/124 (78%)	NA	50/77 (65%)	47/47 (100%)
Receiving ART before hospitalization	73/124 (59%)	NA	45/77 (58%)	28/47 (60%)
CD4 cell count (cells/mm^3)	--	--	--	--
HIV-1 viral suppression	--	--	--	--
Pathogen diagnostics				
Malaria RDT positive	54/237 (23%)	30/116 (26%)	20/76 (26%)	4/45 (8.9%)
Urine TB-LAM positive if PLWH	40/99 (40%)	NA	NA	40/47 (85%)
Cryptococcal ag. positive if PLWH	9/29 (31%)	NA	6/13 (46%)	3/16 (19%)
Influenza PCR positive	14/219 (6.4%)	8/106 (7.5%)	5/71 (7.0%)	1/42 (2.4%)
Outcomes				
Death in hospital	14/241 (5.8%)	4/117 (3.4%)	4/77 (5.2%)	6/47 (13%)

Death at 30 days	49/219 (22%)	10/106 (9.4%)	20/68 (29%)	19/45 (42%)

548 Abbreviations:, KPS: Karnofsky Performance Status, qSOFA: quick Sepsis-related Organ Failure
549 Assessment, PLWH: person living with HIV; WHO: World Health Organization, ART: anti-retroviral
550 therapy, RDT: rapid diagnostic test, TB: tuberculosis, LAM: lipoarabinomannan, PCR: polymerase chain
551 reaction
552 Legend: [a]Dichotomous and categorical variables summarized as counts (proportions), continuous variables
553 summarized as medians (interquartile ranges), n if fewer patients with available data than the total number
554 of patients in the cohort; [b]Systolic blood pressure ≤100mmHg, respiratory rate ≥22 breaths/min, and altered
555 mental status, latter defined using

556

557

558

559

560

561

562

563

564

565

566

567

568

569

570

571

572

573

574

575 **Table 2: Participant characteristics stratified by HIV/TB phenotype in RESERVE-**
576 **U-2-TOR cohort.**

Characteristics [a]	All participants N = 253	HIV - / TB - N = 126	HIV + / TB - N = 73	HIV + / TB + N=54
Demographics				
Female sex	158/253 (62%)	84/126 (67%)	39/73 (53%)	35/54 (65.0%)
Age, years	48 (33, 61)	48 (25, 70)	47 (40, 56)	48 (40, 56)
Mid-upper arm circumference, cm	24 (22, 26)	24 (23, 26)	24 (23, 26)	22 (20, 24)
Illness duration prior to enrollment, days	6 (4, 10)	6 (4, 9)	7 (4, 10)	9 (4, 14)
Clinical signs, lactate, and physiological severity scores				
KPS at hospital admission	60 (20, 70)	70 (20, 80)	60 (40, 70)	50 (20, 70)
Whole-blood lactate, mmol/L	2.4 (1.8, 3.0)	2.4 (1.8, 3.0)	2.4 (1.7, 2.9)	2.4 (2.0, 3.0)
qSOFA score ≥ 2[b]	100/253 (40%)	46/126 (37%)	29/73 (40%)	25/54 (46%)
Modified Early Warning Score	3 (2, 5)	3 (2, 5)	4 (2, 5)	3 (2, 5)
Universal Vital Assessment score	2 (1, 5)	1 (0, 4)	3 (2, 6)	4 (2, 6)
HIV Characteristics				
PLWH	127/253 (50%)	NA	73/73 (100%)	54/54 (100%)
WHO HIV clinical stage 3 or 4	93/127 (73%)	NA	51/73 (70%)	42/54 (78%)
Receiving ART before hospitalization	105/127 (83%)	NA	57/73 (78%)	48/54 (89%)
CD4 count, cells/mm^3	350 (300, 600)	NA	400 (300, 600)	344 (200, 500)
HIV-1 viral suppression	85/120 (71%)	NA	49/68 (72%)	36/52 (69%)
Pathogen diagnostics				
Malaria RDT positive	74/253 (29%)	41/126 (33%)	18/73 (25%)	15/54 (28%)
Urine TB-LAM positive	51/122 (42%)	NA	0/69 (0%)	51/53 (96%)
Cryptococcal ag. positive if PLWH	10/123 (8.1%)	NA	6/70 (8.6%)	4/53 (7.5%)
Influenza PCR positive	14/246 (5.7%)	9/123 (7.3%)	5/72 (6.9%)	0/51 (0%)
SARS-CoV-2 PCR positive	13/246 (5.3%)	8/123 (6.5%)	1/72 (1.4%)	4/51 (7.8%)
Outcomes				
Death in hospital	5/253 (2.0%)	1/126 (0.8%)	1/73 (1.4%)	3/54 (5.6%)

Death at 30 days	51/252 (20%)	11/126 (8.7%)	15/72 (21%)	25/54 (46%)
Death at 60 days	65/252 (26%)	18/126 (14%)	19/72 (26%)	28/54 (52%)

Abbreviations:, KPS: Karnofsky Performance Status, qSOFA: quick Sepsis-related Organ Failure Assessment, PLWH: person living with HIV; WHO: World Health Organization, ART: anti-retroviral therapy, RDT: rapid diagnostic test, TB: tuberculosis, LAM: lipoarabinomannan, PCR: polymerase chain reaction

Legend: [a]Dichotomous and categorical variables summarized as counts (proportions), continuous variables summarized as medians (interquartile ranges), n if fewer patients with available data than the total number of patients in the cohort; [b]Systolic blood pressure ≤100mmHg, respiratory rate ≥22 breaths/min, and altered mental status, latter defined using

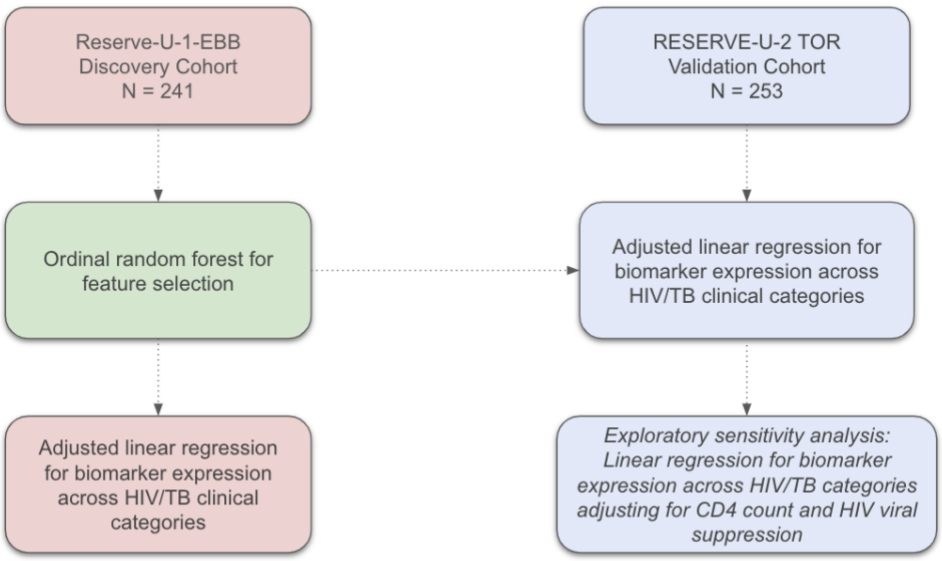

Figure 1. Overview of study design and analytical workflow for proteomic signature discovery and validation.

617

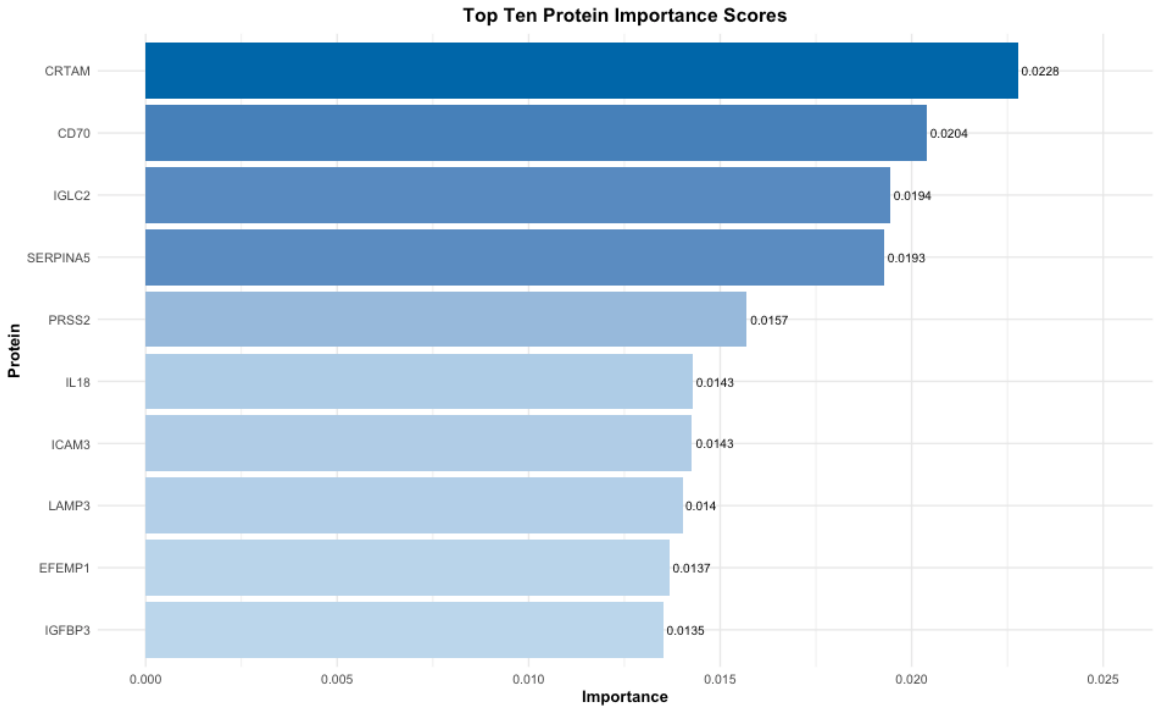

618

619 **Figure 2.** Bar plot of top 10 proteins most predictive of HIV/TB phenotype in the
620 RESERVE-U-1 EBB discovery cohort. Proteins ranked in descending order of
621 permutation-based variable importance as derived from ordinal random forest models (N
622 = 241).

623

624

625

626

627

628

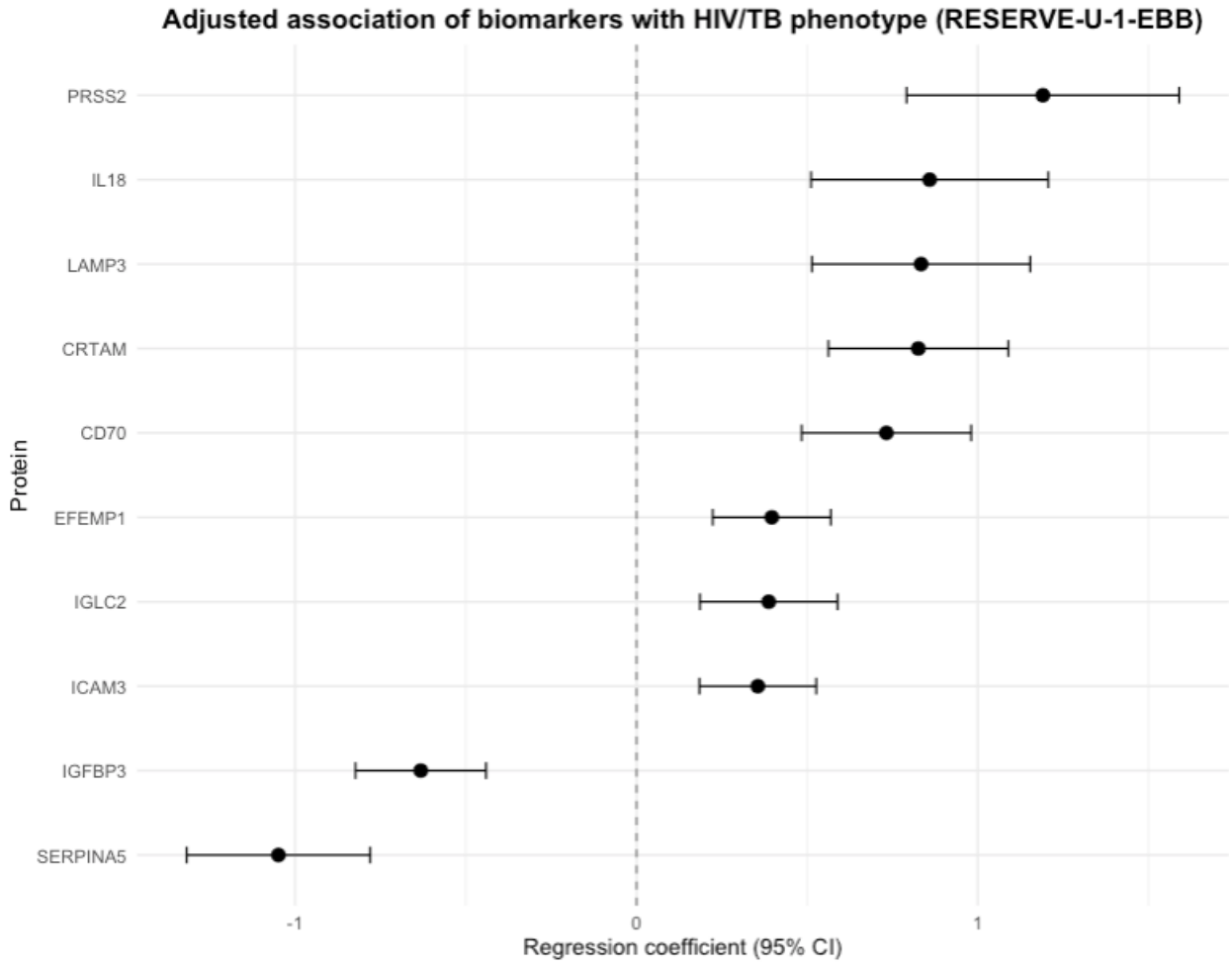

629

630 **Figure 3A**. Forest plot showing adjusted regression coefficients and 95% confidence
631 intervals (CI) for the association between HIV/TB phenotype and protein expression in
632 the RESERVE-U-1-EBB discovery cohort. Coefficients and 95% CIs generated from
633 linear regression models including NPX-quantified protein expression as the continuous
634 outcome and HIV/TB phenotype as an ordinal predictor, adjusted for age, sex, illness
635 duration prior to enrollment, and malaria status (N = 241).

636

637

638

639

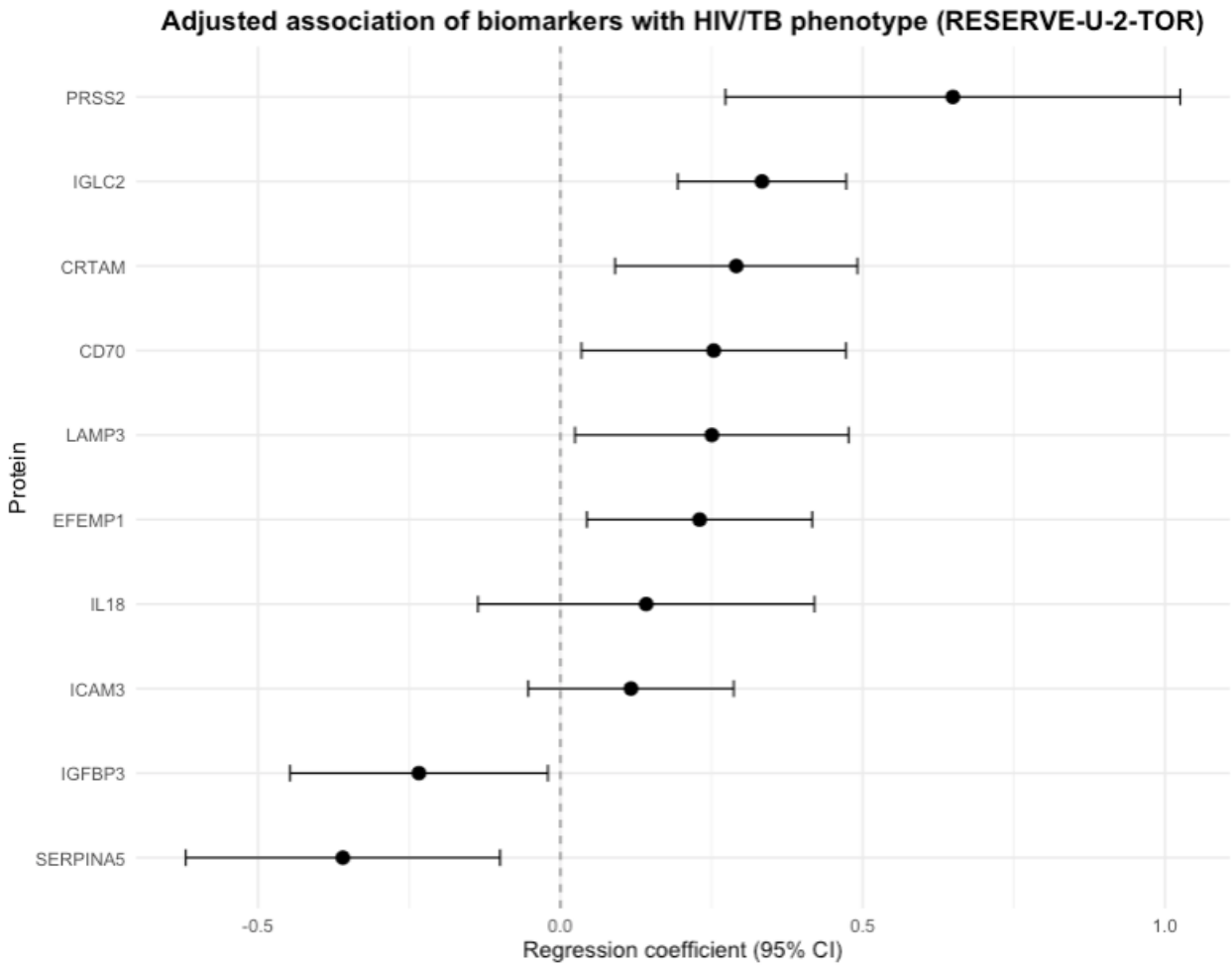

Figure 3B. Forest plot showing adjusted regression coefficients and 95% confidence intervals (CI) for the association between progressive HIV/TB phenotype and protein expression in the RESERVE-U-2-TOR validation cohort. Coefficients and 95% CIs generated from linear regression models including NPX-quantified protein expression as the continuous outcome and HIV/TB phenotype as an ordinal predictor, adjusted for age, sex, illness duration prior to enrollment, and malaria status (N = 253).

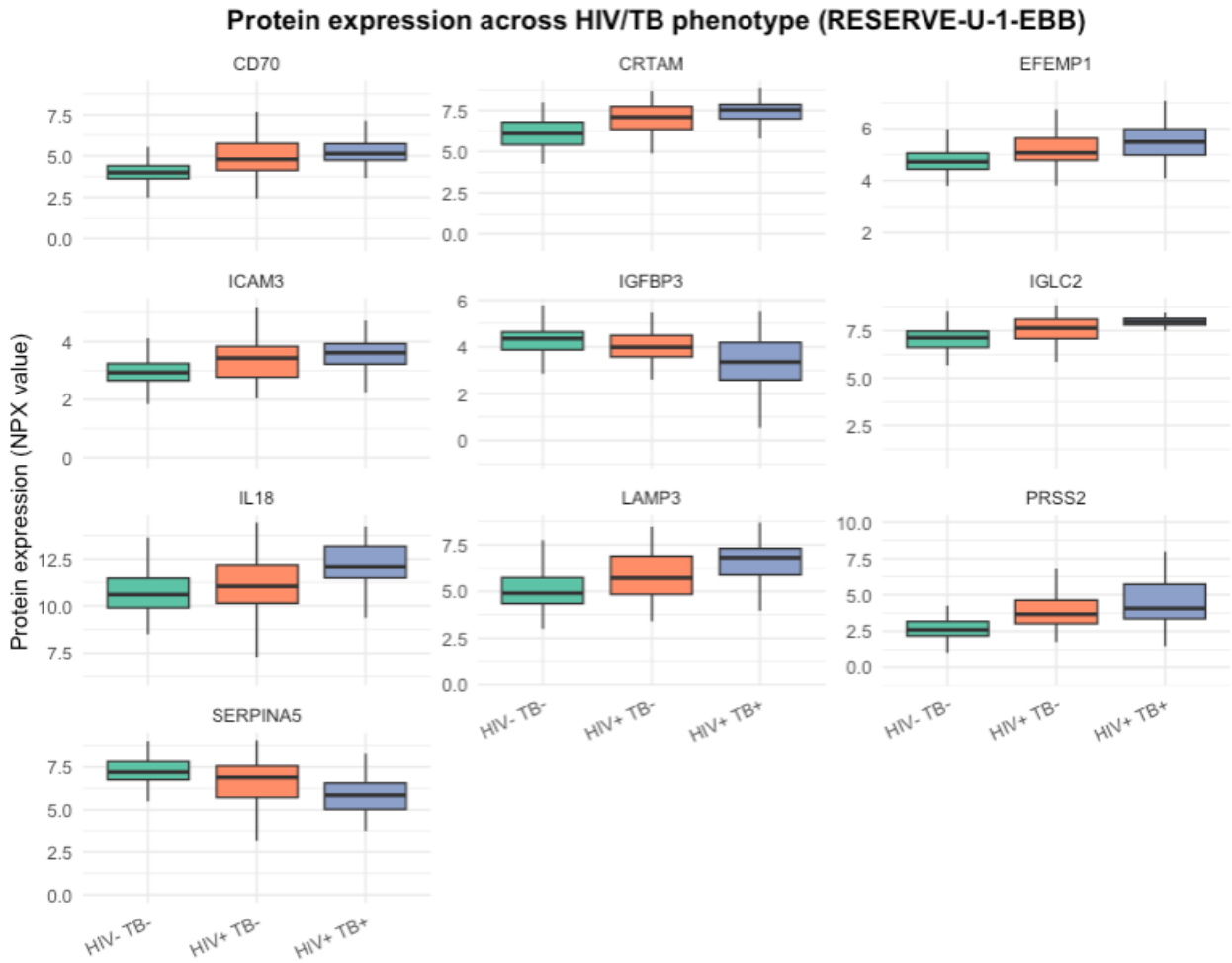

Figure 4A. Boxplots showing distribution of top 10 most predictive proteins across HIV/TB phenotypes in RESERVE-U-1-EBB discovery cohort (N = 241).

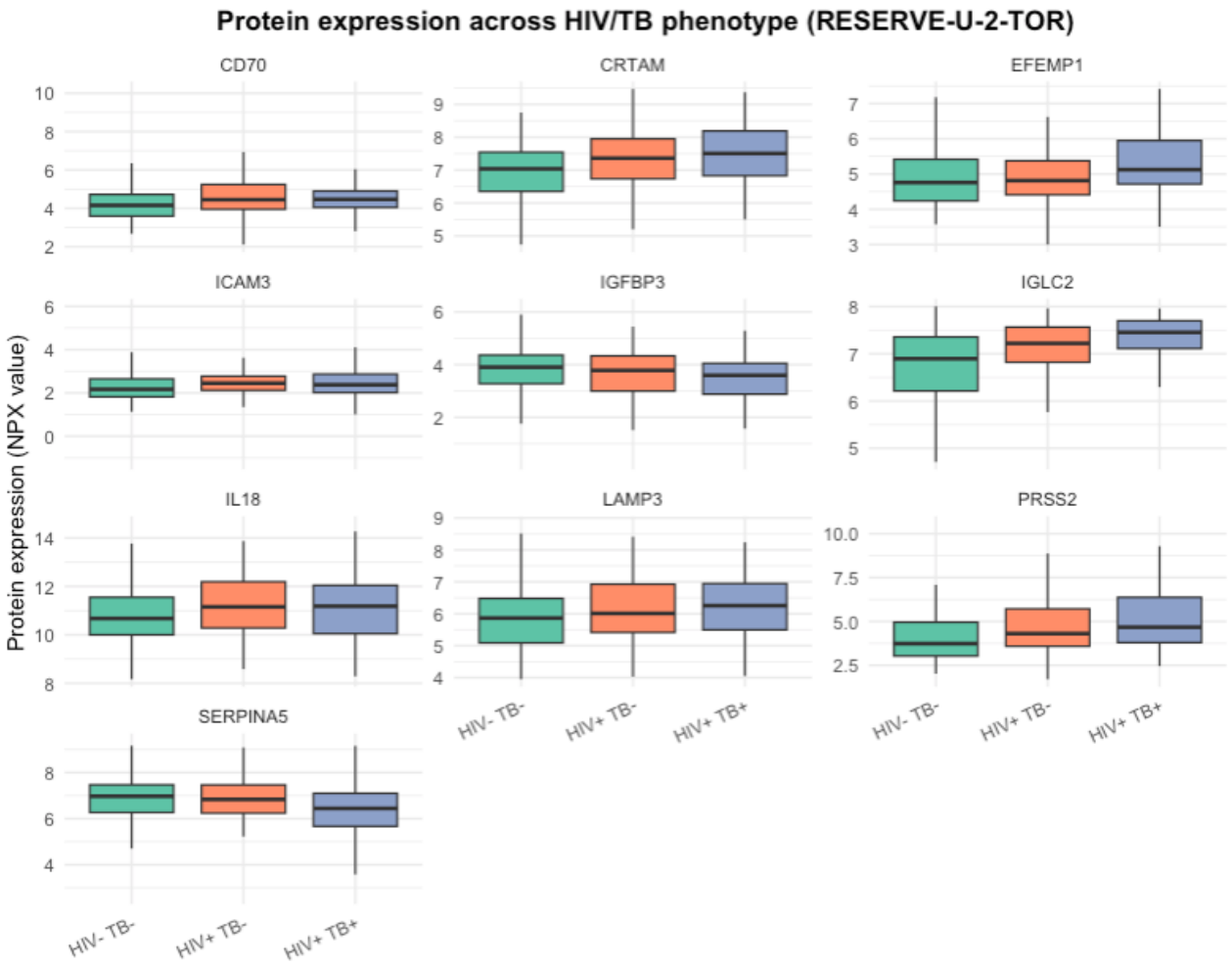

Figure 4B. Boxplots showing distribution of top 10 most predictive proteins across HIV/TB phenotypes in RESERVE-U-2-TOR validation cohort (N = 253).

672

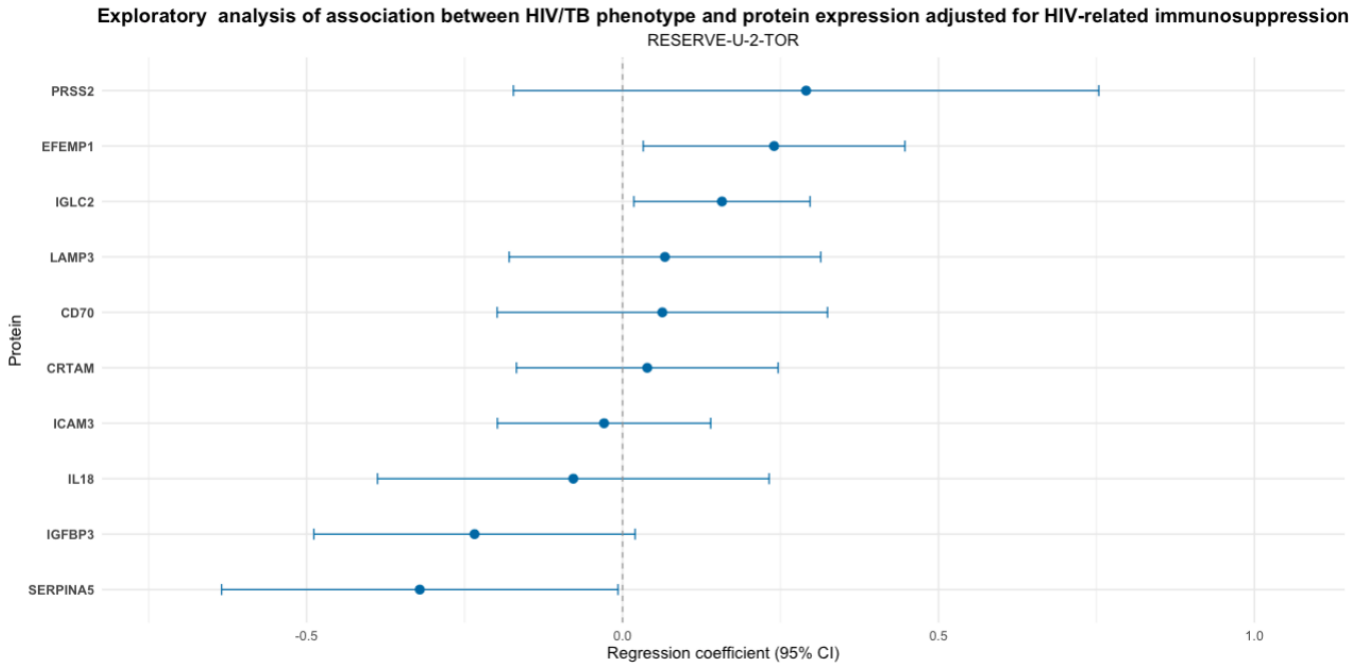

673

674 **Figure 5.** Forest plot of regression coefficients for the association between HIV/TB
675 phenotype and protein expression in PLWH in RESERVE-U-2-TOR cohort. Each model
676 included NPX-quantified protein expression as the continuous outcome and HIV/TB
677 phenotype as an ordinal predictor. Models were adjusted for CD4 count and HIV-1 viral
678 load suppression (N = 127).